Polymer 51 (2010) 6212–6218

Contents lists available at ScienceDirect

Polymer

journal homepage: www.elsevier.com/locate/polymer

Relaxation based modeling of tunable shape recovery kinetics observed under isothermal conditions for amorphous shape-memory polymers

M. Heuchel, J. Cui, K. Kratz, H. Kosmella, A. Lendlein*

Center for Biomaterial Development, Institute of Polymer Research, Helmholtz-Zentrum Geesthacht and Berlin-Brandenburg-Center for Regenerative Therapies (BCRT), Kantstrasse 55, 14513 Teltow, Germany

ARTICLE INFO

Article history:
Received 1 September 2010
Received in revised form
22 October 2010
Accepted 26 October 2010
Available online 2 November 2010

Keywords:
Shape-memory polymer
Stress relaxation
Viscoelastic model

ABSTRACT

Polymers, which allow the adjustment of shape-memory properties by variation of physical parameters during programming, are advantageous to their counterparts requiring synthesis of a new material.

Here we explored the stress relaxation behaviour of polyurethane (PEU) based shape-memory polymers at temperatures from 0 °C to 80 °C and different strain values from 100% to 250%. The obtained relaxation curves could be well described by a modified Maxwell–Weichert model of two Maxwell units and a spring. The stress relaxation results in a combination of a slow and a fast decaying process. For modeling the isothermal recovery of recently introduced PEU composite scaffolds at 37 °C the fast relaxation could be neglected resulting in a model of a standard linear solid, which was in good agreement with the experimental data.

The presented modeling approach might be helpful to define design criteria for self sufficiently moving scaffolds within a knowledge-based development process.

1. Introduction

Shape-memory polymers (SMPs) [1–4] constitute a group of mechanically active polymers [5,6], which have attracted widespread interest, because they are able to perform single, dual or multiple shape changes [7–9] when activated by external stimuli (e.g. heat or light). The thermally induced shape-memory functionality results from the combination of a polymer's molecular architecture, morphology and a specific multi step processing technology named shape-memory creation procedure (SMCP) or programming, where the temporary shape is created [2]. On the macroscopic level shape-memory properties are typically quantified in cyclic, thermomechanical tensile experiments, which consist of an SMCP followed by a recovery module either under stress-free or constant strain conditions [10]. SMPs are lightweight materials, which are easy to process and their properties can be tailored to the requirements of the desired application by adjusting the polymer's molecular structure (e.g. change in switching segment length or chemical composition) requiring synthesis of a new material [11–14] or the variation of the composition of blends or composites [15–17]. Furthermore, the variation of physical parameters applied during SMCP, like the applied strain ε_m [18,19] or the programming temperature T_{prog} [9,19–22] where the material was deformed as well as the heating rate during the recovery process can influence the shape-memory behaviour [23]. Such SMPs with tunable properties are of significant scientific and technological interest as their shape-memory properties can be easily adapted without synthesizing a new polymer, which will substantially broaden the applicability of these materials. Besides the understanding of the structure–function-relation of individual SMP materials modeling approaches, which enable the prediction of thermomechanical properties of SMPs are essential to realize industrial or medical applications. Here within the last decade two main routes were followed. The first included the application of existing linear viscoelastic models consisting of coupled spring, dashpot, and frictional elements. Other researcher concentrated on the development of rather complex models (constitutive equations) for specific molecular transitions related to the shape-memory effect in polymer systems, i.e. the glass transition [24–26] or the melting transition [27–29]. More recently theoretical models and frameworks have been developed, which address the description and prediction of tunable shape-memory properties [21,30].

In this work, we want to explore, whether a theoretical model can be developed, which is able to describe the different shape recovery kinetics observed for radiopaque polyether urethane (PEU) based 3D substrates under isothermal conditions (37 °C in water), which could be adjusted by variation of the programming temperature (T_{prog}) applied during SMCP [20]. Such active substrates/scaffolds can self sufficiently change in pore size and geometry, when exposed

* Corresponding author.
E-mail address: andreas.lendlein@hzg.de (A. Lendlein).

0032-3861/$ – see front matter © 2010 Elsevier Ltd. All rights reserved.
doi:10.1016/j.polymer.2010.10.051

to physiological conditions and intended for stimulation of mechano-sensitive cells in vitro or in vivo. The pores of these active substrates were programmed at different T_{prog} by deformation of the original, square shape with a pore area of ca. 2.5 mm^2 to a circular shape with a pore area in the range of 6.0–8.5 mm^2, while the temporary shape was fixed at 0 °C in ice water. By increasing the applied T_{prog} the recovery time under isothermal conditions (37 °C in water) could be increased from 1 h to 6 h.

Thermoplastic PEU can be synthesized from methylene bis-(*p*-cyclohexyl isocyanate) (H_{12}MDI), poly(tetramethylene glycol) (PTMEG), and 1,4-butanediol (1,4-BD) and exhibit a pronounced glass transition ($T_{g,mix}$) in the range from 20 °C to 90 °C, which is related to a mixed phase of H_{12}MDI/1,4-BD hard domains and H_{12}MDI/PTMEG soft domains. PEU was selected because $T_{g,mix}$ can easily be adjusted by variation of the hard to soft segment ratio [19,20,31]. PEU and composites thereof exhibit excellent shape-memory properties where the $T_{g,mix}$ is utilized as switching domain [32–35]. Furthermore a temperature-memory effect was reported for PEU with 58 wt % hard segment content, when T_{prog} was varied within $\Delta T_{g,mix}$ [19].

Here, we concentrate on investigation and modeling of the thermodynamic process of the stress relaxation of PEU, which were deformed to a strain (ε) in the range from 100% to 250% at varied temperatures (T_{prog}) between 0 °C (glassy state) and 80 °C (viscoelastic state), within a relaxation time of 6 h based on a series of Maxwell models in parallel.

2. Materials and methods

2.1. Materials

Aliphatic polyether urethane (PEU) was purchased from Neveon (Wilmington, MA, USA) as Tecoflex® EG72D and used without further purification. The amorphous multiblock copolymer was synthesized from methylene bis(*p*-cyclohexyl isocyanate) (H_{12}MDI), poly(tetramethylene glycol) (PTMEG, $M_n = 1000$ g mol^{-1}) and 1,4-butanediol (1,4-BD).

2.2. Sample preparation

PEU granules were dried for 12 h at 130 °C prior to the processing and test specimens of type DIN 50125 (L0 = 40 mm, width = 5 mm, thickness = 2 mm) were fabricated using an injection moulding machine (type: Allrounder 270U-Arburg, Lossburg, Germany). The injection moulding temperature was 200 °C and the mould temperature was 20 °C. The injection pressure was 700 bar, while the holding pressure decreased from 1000 bar to 400 bar within a holding time of 1.42 s.

2.3. Stress relaxation experiments

Stress relaxation experiments were carried out on a Zwick Z005 (Zwick, Ulm, Germany) tensile tester equipped with a temperature controlled thermo chamber (Eurotherm Regler, Limburg, Germany). The test specimen was fixed between the clamps and the temperature (programming temperature T_{prog}) was equilibrated at 0, 25, 37, 50, 60, 70 or 80 °C for a time period of 10 min. Then the sample was deformed at T_{prog} to a fixed elongation $\varepsilon_m = 100\%$, 150%, 200% or 250% with a strain rate of 5 mm min^{-1}. Afterwards, the strain was kept constant for 6 h at identical temperatures to allow stress relaxation.

2.4. Modeling of stress relaxation processes

An introduction into the theoretical description of stress relaxation processes can be found, e.g. in the text book of Ward and Sweeney [36]. For the modeling of stress relaxations of polymers one uses a set of Maxwell units in parallel representing n different relaxation processes in the polymer. Every process is characterized by a different relaxation time τ. The model is also named Maxwell–Weichert model [37]. It should be noted that the assumption of an infinite number of different relaxation times would result in a spectrum of relaxation times. We use in the following a modified Maxwell–Weichert model with only n = 3 units (see Fig. 1) were the third unit consists only of a spring representing a long time elastic component (One could imagine that the dashpot of the third unit was filled with a low viscosity fluid, and shows an effectively instantaneous response).

For the stress relaxation $\sigma(t)$ of a single Maxwell unit, consisting of a spring and a dashpot in series, the following relation can be derived

$$\sigma(t) = \varepsilon E \exp\left(-\frac{t}{\tau}\right) \quad (1)$$

where $\varepsilon = (L - L_0)/L_0$ is the strain, E is the spring constant, and $\tau = \eta/E$ is the characteristic relaxation time, expressed as a ratio of the viscosity of the dashpot and spring constant of the elastic spring. For a series of n Maxwell units in parallel, all at strain ε, the stress relaxation is

$$\sigma(t) = \varepsilon \sum_{i=1}^{n} E_i \exp\left(-\frac{t}{\tau_i}\right) \quad (2)$$

where E_i and τ_i refer to the ith Maxwell unit. Often one introduces the stress relaxation modulus, $G(t) = \sigma(t)/\varepsilon$, and obtains then for a system consisting of three Maxwell units in parallel, where the third consists of only a spring representing the long time elastic behaviour the following model relation

$$G(t) = \frac{\sigma(t)}{\varepsilon} = E_1 \exp\left(-\frac{t}{\tau_1}\right) + E_2 \exp\left(-\frac{t}{\tau_2}\right) + G_r \quad (3)$$

which is used in the following discussion of the presented relaxation experiments.

3. Results and discussion

The chemical structure of PEU consists of H_{12}MDI/1,4-BD hard segments and H_{12}MDI/PTMEG soft segments, in which the content of H_{12}MDI/1,4-BD was 58 wt% according to the calculation from ^{1}H NMR spectroscopy [20]. As previously described [32], three relaxation processes could be distinguished by dynamic mechanical analysis (DMTA) at varied temperatures (Fig. 2, DMTA curves with marked region for T_{prog}-range) from the plot of mechanical loss factor tanδ, which is the ratio of loss modulus (E'') to storage modulus (E'), against temperature.

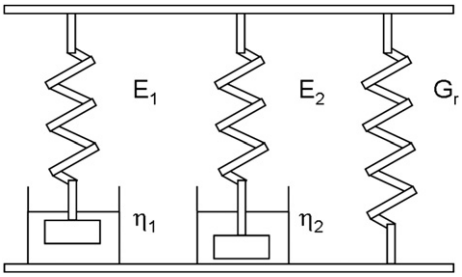

Fig. 1. Modified Maxwell–Weichert model consisting of two Maxwell units and a third spring in parallel. Deleting Maxwell unit "1" leads to the model of a *standard linear solid* (SLS).

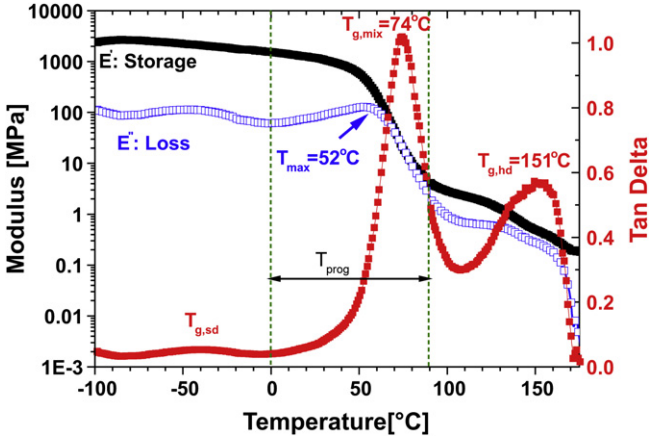

Fig. 2. DMTA curves of PEU including storage modulus E', loss modulus E'' and tan delta. Measurement with Eplexor 25 N, Gabo at a frequency of 10 Hz and a heating rate of 2 K/min. Additionally the experimental T_{prog}-range is marked.

The first relaxation process in the temperature range from −80 °C to −10 °C was attributed to the glass transition of the soft domains ($T_{g,sd}$), and the second process with a pronounced peak maximum $T_{g,mix} = 73$ °C reflected the glass transition of the mixed phase of hard and soft segments. At high temperatures between 110 °C and 170 °C, a third transition with peak maximum $T_{g,hd} = 151$ °C was found, which was related to the softening temperature of the hard domains. The two vertical lines in Fig. 1 indicate the temperature range of the relaxation experiments. Therefore relaxation processes are investigated in a material stage were the soft domains of the PEU are in a rubbery state, hard domains of the PEU still exist, and where with increasing temperature an increasing amount of mixed phase migrates from a glassy to a rubbery state. If we assume that the composition of the different domains remains constant in the considered temperature range, in a sense PEU can be considered in the following relaxation experiments like a homogeneous amorphous polymer showing a single glass transition.

Stress relaxation experiments of PEU were conducted at seven different T_{prog} ($T_{prog} = 0$, 25, 37, 50, 60, 70 or 80 °C) for strain values of $\varepsilon_m = 100\%$, 150%, 200% or 250%. Fig. 3a displays for the largest strain $\varepsilon_m = 250\%$ at $T_{prog} = 25$, 37, 60, and 80 °C the typical stress relaxation curves measured with the tensile tester.

In Fig. 3a, the time $t = 0$ corresponds to the start of the stress-strain experiment. At a strain rate of 5 mm min^{-1} it takes 20 min to elongate a sample of initially 40 mm to 140 mm corresponding to a strain value of 250%. During this time period the sample may pass through three regions, (I) a linear elastic region, (II) a "yield region", where first very fast relaxation processes start, and from yield point up to an inflection point the extension continues easier, and (III) a "post-yield region" where the tensile stress again strongly increases. The maximum tensile stress at the final extension is called the initial stress σ_0 for the relaxation experiment. In Fig. 3a it is seen for the curves at all shown $T_{prog} = 25$, 37, and 60 °C as the pronounced peak maximum at $t = 20$ min. After the final elongation ε_m is reached, this ε-value is kept constant, and only then in the classical meaning stress relaxation starts, seen as a characteristic decrease of the tensile stress with time. It should be mentioned that in all experiments over the observation time period the stress relaxed not to zero, but to a finite value $\sigma_r > 0$. Fig. 3b presents a plot of initial stresses σ_0 as function of strain ε for all programming temperatures T_{prog}. At a certain T_{prog}, the initial stress increases with strain ε_m, and at constant elongation, the initial stress becomes drastically smaller with increasing T_{prog}.

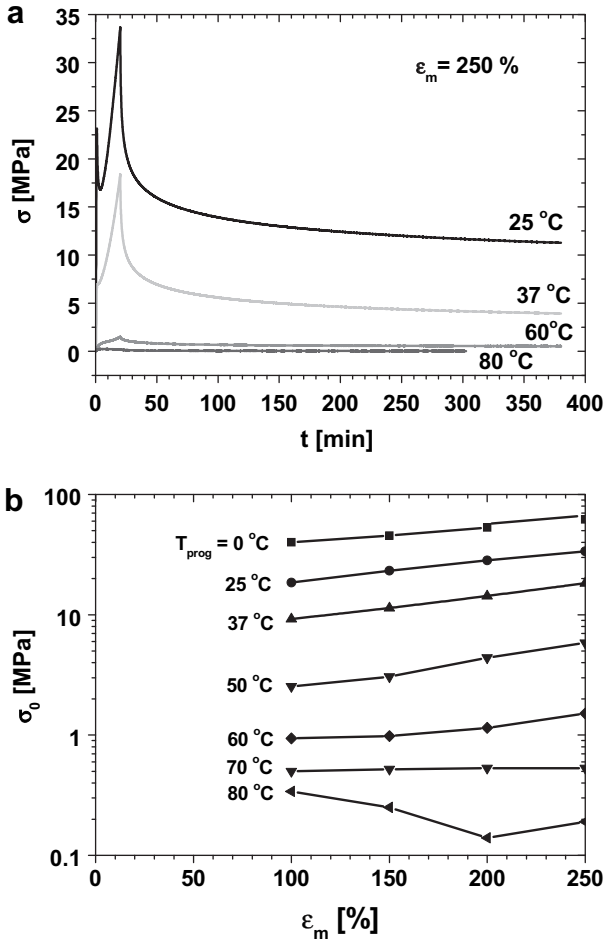

Fig. 3. Relaxation experiments for PEU. a) Typical relaxation curves at $\varepsilon_m = 250\%$ and $T_{prog} = 25$, 37, 60, and 80 °C. b) Stress σ_0 at the beginning of the relaxation process for different strain values ε_m.

The principal modeling approach of the relaxation curves based on Eq. (3) is presented in Fig. 4 for an example ($T_{prog} = 25$ °C, $\varepsilon_m = 250\%$).

For the modeling only the relaxation part of the tensile test curve (see in Fig. 3a, the decreasing curves for $t \geq 20$ min) is taken, the tensile stress is transformed to a relative stress $\sigma(t)/\sigma_0$, so that the modeled relaxation process starts at $t = 0$ with the initial value

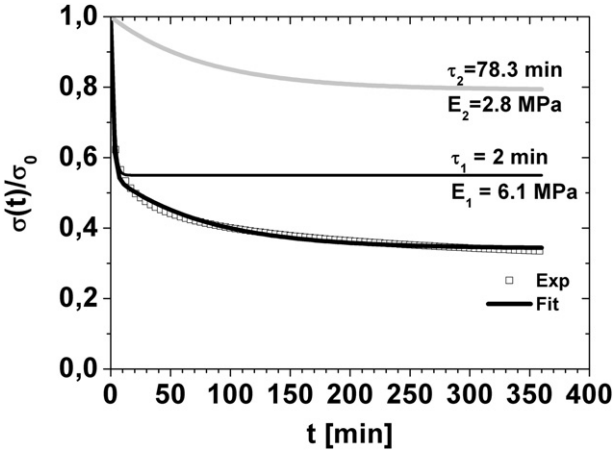

Fig. 4. Principal modeling approach of a relaxation curve of PEU with the modified Maxwell–Weichert model (see Fig. 1 and Eq. (3)) for $T_{prog} = 25$ °C and $\varepsilon_m = 250\%$.

of 1.0. The experimental data are fitted to the presented Maxwell–Weichert model (Eq. (3)) with a numerical least error square method to obtain the following five unknown parameters: G_r, the relaxed stress, E_1 and E_2, the moduli of the springs in Maxwell units "1" and "2", and τ_1 and τ_2, the relaxation times of the dashpots in the two Maxwell units. Fig. 4 shows (see thick black line) that with these 5 parameters the experimental relaxation data may be very well described. Fig. 4 contains also the individual relaxation curves of the two single Maxwell units. Unit "1" relaxes fast. In the example of Fig. 4 the relaxation time τ_1 has a value of 120 s, where unit "2" relaxes more than one order of magnitude slower (in the example $\tau_2 = 4700$ s). The fast relaxation process (unit "1", thin black line) dominates the initial period of the relaxation process, and then the slow process (unit "2", thick grey line) is characteristic for the further relaxation of the PEU sample. Fig. 4 shows also clearly that at least two Maxwell units are necessary to describe the relaxation processes. More examples for fits of the experimental stress relaxation curves are presented in Fig. 5.

Fig. 5a shows the fits of the relaxation curves for the four elongations at $T_{prog} = 25$ °C. The model describes the experimental curves very well. Additionally, one sees the influence of the strain on the relative relaxation. The initial decrease in stress is rather independent on the value of the strain, but the limiting value of the relaxed stress increases with strain. At constant strain (see Fig. 5b) the situation is more complex. The initial strong drop of stress changes with temperature, but also the terminal values of the relaxed stress after long observation times changes not proportional with the programming temperature. But in all cases the fit of the experimental curves by the model is satisfactorily. It should be noted that the scatter of the experimental points in $\sigma(t)/\sigma_0$-representation of data for the $T_{prog} = 80$ °C curve is due to the resolution of the tensile tester. The initial stress has "only" a value of 0.19 MPa.

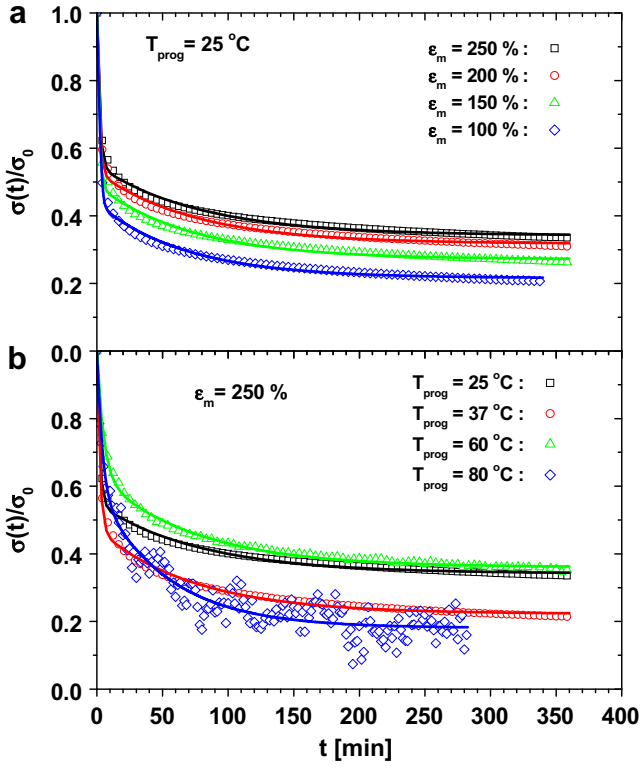

Fig. 5. Modeling of experimental stress relaxation curves for PEU with Eq. (3). a) at $T_{prog} = 25$ °C for $\varepsilon_m = 100$, 150, 200 and 250%. b) at $\varepsilon_m = 250\%$ and $T_{prog} = 25$, 37, 60, and 80 °C.

The obtained parameter values are listed in Table S1 as supplementary data (see Appendix).

We see that e.g. the relaxed modulus G_r does only slightly change with strain, but depends strongly on the programming temperature T_{prog}. Following a proposal in a recent work [38], we tested the possibility that the remaining stress σ_r has its origin in an "internal network" stretched in the drawing process. The affine network model for stresses in uniaxial deformations predicts then the following relation

$$\sigma_r = G_r^{eff}\left(\lambda^2 - 1/\lambda\right) \quad (4)$$

where $\lambda = L/L_0$ is the elongation and G_r^{eff} would be an effective modulus for the PEU. Fig. 6 shows (for $T_{prog} > 0$ °C) the plot of the relaxed stresses σ_r versus $\lambda^2 - 1/\lambda$, and the fit of these data with Eq. (4).

The obtained moduli G_r^{eff} are presented in Table 1.

Except the lowest programming temperature ($T_{prog} = 0$ °C) the model describes the data well. Between $T_{prog} = 25$ and 70 °C, the slope, i.e. the effective modulus decreases with increasing T_{prog}. This can be interpreted as a reduction of the number of effective crosslinks in the material. As effective crosslinks we assume next to hard segment domains, the glassy domains in the pronounced mixed phase of the PEU, whose weight content decreases with increasing T_{prog}. At $T_{prog} = 0$ °C PEU is in the glassy state (see. Fig. 2), where also a certain plastic deformation has to be considered, which could be the reason for the deviation from the model based on Eq. (4).

The initial stress relaxation modulus $G_0 = G(t = 0) = \sigma(t = 0)/\varepsilon$ shows a slight decrease with extension from 100% to 250% (not shown here). Most pronounced is the change with strain for the spring constant E_1 for the fast Maxwell unit "1" at low temperatures. At $T_{prog} = 80$ °C, E_1 changes from 16.6 MPa to 8.4 MPa, i.e. around 50%.

Next we look at the temperature dependency of the modeling parameters. In this way we only obtain information about the pronounced mixed phase, characterized by $T_{g,mix} = 73$ °C determined by DMTA as maximum in the tan δ-curve (see Fig. 2); where the mixed phase composition is assumed as unchanged in the investigated temperature range. Fig. 7a and b presents the obtained relaxation times and the elastic moduli as function of the inverse temperature, the common way to detect thermal activated processes, and to determine thermal activation energies.

The fitted τ-values show a characteristic change (drop) above the glass transition of the mixed phase ($T_{g,mix} = 74$ °C). From $T_{prog} = 0$ °C up to 70 °C, the τ_2-values (for the "slow" relaxation

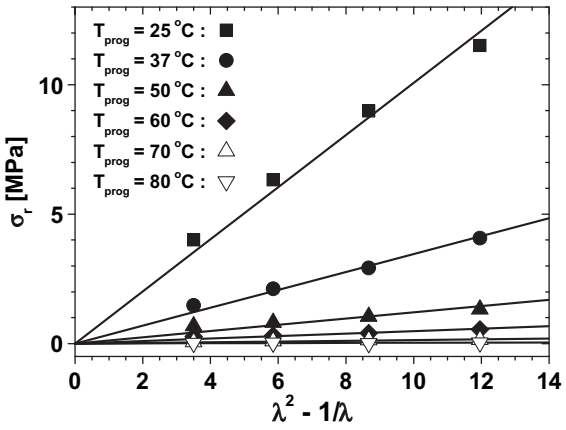

Fig. 6. Relaxed stress σ_r as function of $(\lambda^2 - 1/\lambda)$ to test the assumption of an effectively internal network. Lines are linear fits $\sigma_r = G_r^{eff}(\lambda^2 - 1/\lambda)$.

Table 1
Best fit parameter values for the effective modulus G_r^{eff} in the relation $\sigma_r = G_r^{eff}(\lambda^2 - 1/\lambda)$ for PEU elongated at different T_{prog}-values.

T_{prog} [°C]	G_r^{eff} [MPa]	Correl. Coeff. R^2
0	2.89 ± 0.30	0.959
25	1.01 ± 0.30	0.996
37	0.35 ± 0.01	0.996
50	0.12 ± 0.01	0.970
60	0.048 ± 0.004	0.974
70	0.014 ± 0.001	0.980
80	0.003 ± 0.001	0.773

process) are rather constant. A similar behaviour can be also seen for the "fast" relaxation process on a much shorter time scale. From 0 °C up to 37 °C, τ_1 is relatively constant, and increases then up to 70 °C, this is also the range where storage and loss modulus in the DMTA plot (see Fig. 2) decrease strongly.

A different temperature dependency is observed for the elastic moduli. As Fig. 7b shows, all three parameters E_1, E_2 and G_r decrease significantly (over about 3 orders of magnitude) over the T_{prog}-range from 0 °C up to 80 °C. Here, one can assume a thermally activated process.

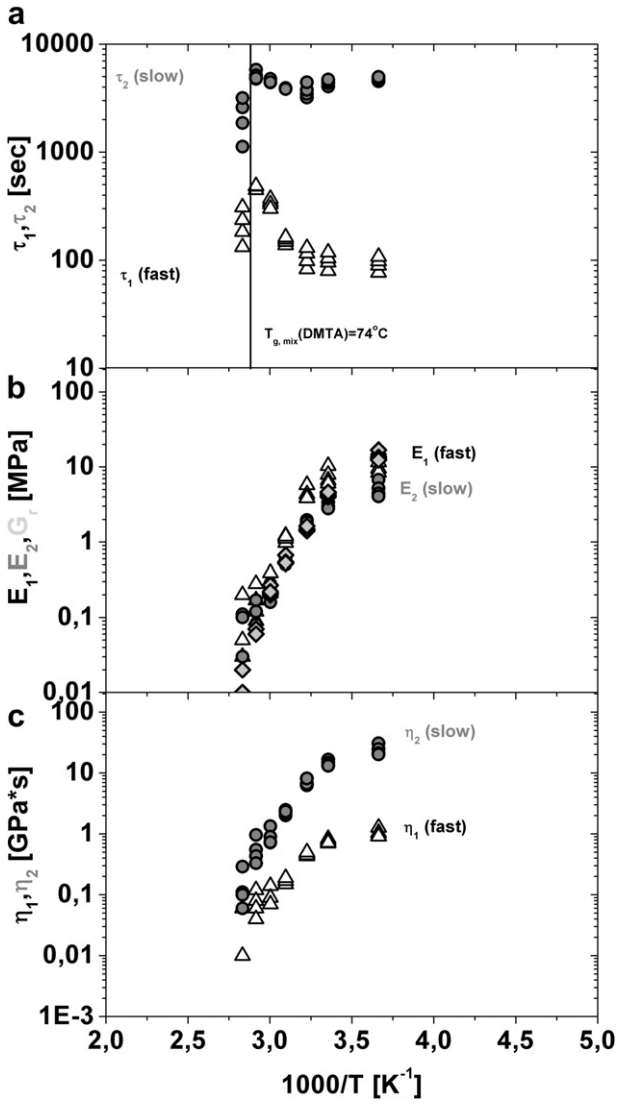

Fig. 7. Temperature-dependency of obtained model parameters: a) relaxation times τ_1 and τ_2; b) moduli E_1, E_2 and G_r; c) viscosities $\eta_i = \tau_i E_i$, i = 1,2.

The single T-dependencies of either the relaxation times (rather independent of T) and the spring constants (strong dependency on T) determine the T-dependency of the viscosities of both Maxwell units presented in Fig. 7c. It is $\eta_i = \tau_i E_i$, i = 1,2, and the viscosities for both ("fast" and "slow") relaxation processes show the same strong T-dependency as the three mechanical moduli.

We discuss now consequences of the stress relaxation behaviour of the PEU in a shape-memory cycle, esp. the free recovery of such a material. After the previous discussion, we can assume that already after about 2 min the "fast" relaxation process "1" is decayed so that the stress–strain behaviour of the material in all subsequent processes, e.g. in a shape-memory cycle, are bound to a simpler model. So, it should be sufficient to consider only the Maxwell unit "2" for the slow relaxation in parallel with the spring of the relaxed stress G_r (see Fig. 1). This simplified model is a common mechanical model: the *standard linear solid* (SLS). The stress–strain relationship for the standard linear solid looks the following [39]:

$$\sigma + \tau_2 \frac{d\sigma}{dt} = G_r \varepsilon + (G_r + E_2)\tau_2 \frac{d\varepsilon}{dt} \tag{5}$$

where the variables of Fig. 1 have been used. In the following, we are interested on a relation for recovery experiments as part of a shape-memory cycle for the PEU material. After samples are stretched at the programming temperature, the samples are cooled down to a very low temperature, then the stress is released and one observes e.g. a stress free recovery of the sample under isothermal conditions. In the stress-free case ($\sigma, \dot{\sigma} = 0$) the differential Eq. (5) can be integrated and gives the following approximation for the time dependent strain development $\varepsilon(t)$ in a stress free recovery under isothermal conditions:

$$\varepsilon(t) = \varepsilon_d \exp\left(-\frac{G_r}{G_r + E_2}\frac{t}{\tau_2}\right) \tag{6}$$

where ε_d is the deformed strain of the (programmed) sample after relaxation at the beginning of the recovery experiment at $t = 0$. It is always $\varepsilon_d \le \varepsilon_m$. With Eq. (6) for the strain recovery it is also possible to calculate in the framework of the model values for the *apparent shape recovery rate* R_r^{app}

$$R_r^{app} = \frac{\varepsilon_d - \varepsilon(t)}{\varepsilon_d} \tag{7}$$

This relation is similar to Eq. (5) of Ref. [20] but it should be noted that in Ref. [20] the apparent shape recovery rate was defined with respect to area values. If one assumes that the area changes were isotropic, then the area of the originally square shaped pore should correspond in our kinetic modeling consideration to the situation of a one dimensional model where $L = 0$, i.e. $\varepsilon = 0$.

A qualitative trend of the time dependent recovery rate R_r^{app} for samples stressed before on different T_{prog}-values can be seen in Fig. 8 with parameter values of G_r and E_2 (see Supplementary data) for the respective temperatures T_{prog}, and for τ_2 the value for $T_{prog} = 37$ °C was used.

It can be seen from Fig. 8 that the model is qualitatively capable to present the T_{prog} influence on an isothermal recovery calculation. However, with Eq. (6) and the respective parameters (see Supplementary data), it was not possible to predict the experimental recovery data of Ref. [20], which were discussed in the introduction. But it is possible to fit these experiments with a simplified model based on Eq. (6).

$$\varepsilon(t) = \varepsilon_d^* \exp\left(-\frac{t}{\tau^*}\right) \tag{8}$$

The model contains two fit parameters. ε_d^* represents a deformed strain of the sample at the beginning of the recovery

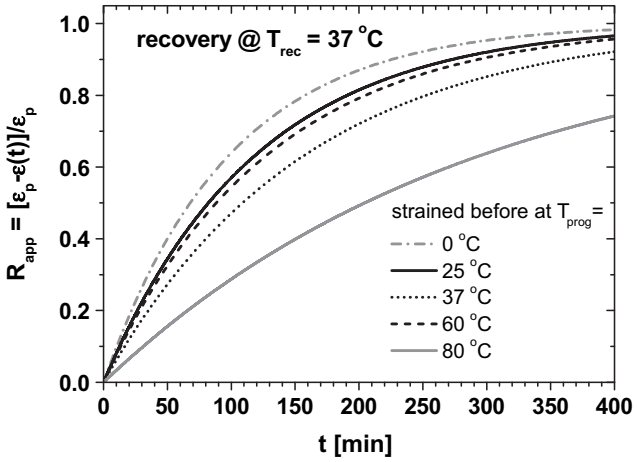

Fig. 8. Prediction of free recovery rate R_r^{app} for PEU at $T_{rec} = 37\ ^\circ C$ based on the model Eq. (6). For respective parameter values see Supplementary data.

under *isothermal* conditions (in contrast to ε_d). The effective relaxation time τ^* depends on both the recovery temperature T_{rec} and on the programming temperature T_{prog}. This special dependency becomes clear by comparison Eq. (6) with the solution of the SLS model Eq. (8). The effective relaxation time τ^* is proportional to $\tau_2(T_{rec})$ a function of the recovery temperature, and a factor $(G_r+E_2)/G_r$ which depends on T_{prog}. The motivation originates from the previously reported experimental results [20]. Under isothermal recovery conditions it was observed that a complete recovery with R_r^{app} values >98% only occurred, when the applied T_{prog} was close to the recovery temperature T_{rec}, whereas for higher T_{prog} lower R_r^{app} values up to 88% were obtained. As a complete recovery could be achieved for higher T_{prog} by increasing T_{rec}, here we introduced a second fit parameter ε_d^* which reflects the final R_r^{app} values reached at the recovery temperature T_{rec}. For the apparent shape recovery rate R_r^{app} in Eq. (7) we obtain now an equation with two fit parameters, the effective relaxation time τ^* and the ratio $\varepsilon_d^*/\varepsilon_d$.

$$R_r^{app} = 1 - \frac{\varepsilon_d^*}{\varepsilon_d} \exp\left(-\frac{t}{\tau^*}\right) \tag{9}$$

The fit of the experimental data of Ref. [20] is presented in Fig. 9.

The obtained best fit parameter values for the effective correlation time τ^* and the final relative recovery $\varepsilon_d^*/\varepsilon_d$ are presented in Table 2.

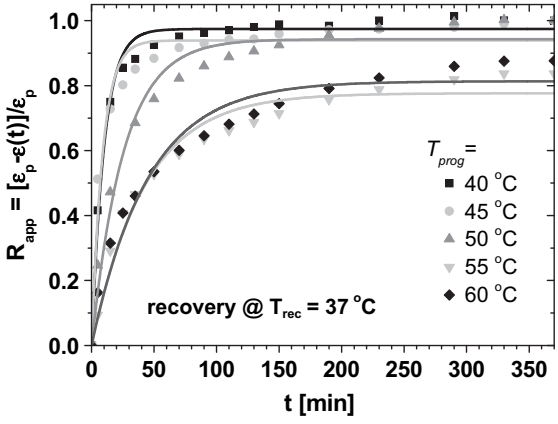

Fig. 9. Fit of experimental free recovery rate R_r^{app} values at $T = 37\ ^\circ C$ for PEU based scaffolds which were programmed at different T_{prog}-values (see Fig. 6 of Ref. [20]) using model Eq. (9)).

Table 2
Best fit parameter values $\varepsilon_d^*/\varepsilon_d$ and τ^* for the effective free recovery model Eq. (9) applied to experimental data (Ref. [20]) for $T_{rec} = 37\ ^\circ C$ for different T_{prog}-values.

T_{prog} [°C]	$\varepsilon_d^*/\varepsilon_d$	τ^* [min]	Correl. Coeff. R^2
40	0.97	9.9	0.983
45	0.94	8.7	0.925
50	0.94	25.6	0.964
55	0.78	42.3	0.964
60	0.81	45.0	0.952

As shown in Table 2 high values of correlation coefficients above 0.93 were observed for all T_{prog} in the range from 40 °C to 60 °C and the effective correlation time increased from ca. 10 min to 45 min with increasing T_{prog}, which is in agreement with the observation in Ref. [20]. The values of $\varepsilon_d^*/\varepsilon_d$ express the differences of recovery kinetics between a 3D system (the scaffold) and the uniaxial model system.

The fit also demonstrates that the recovery kinetics under isothermal conditions can be tailored by variation of T_{prog} in the two-dimensional deformation, where higher recovery was realized at programming temperatures T_{prog} close to T_{rec}, which could be explained by the temperature-memorizing capability of the material [19], where the recovery rate at a fixed temperature was influenced by T_{prog} and could be accelerated when the recovery temperature was adjusted close to T_{prog}.

4. Conclusions

Based on the isothermal stress relaxation behaviour of amorphous polyether urethanes (PEUs) at T_{prog} between 0 °C and 80 °C we propose a kinetic model approach for description of the shape-recovery characteristics of actively moving PEU composite scaffolds. The obtained relaxation curves could be well described by a five parameter Maxwell–Weichert model of two Maxwell units plus a third spring in parallel. The last spring describes the relaxed stress and can be assigned to an internal network stretched in the drawing process. The stress relaxation results in a slow and a fast process, which decays already after a few minutes during SMCP. For this reason the model could be simplified to a standard linear solid (Maxwell unit and spring) approach for description of the experimental data previously reported for isothermal recovery of PEU composite scaffolds, which were intended for autonomous mechanical stimulation of cells in vitro or in vivo.

The here “experimentally extracted” relaxation model is similar to viscoelastic models applied for the description of the shape recovery behaviour. The model of Lin and Chen [14] assumed a set of two parallel Maxwell units representing the “reversible phase” and the “fixed phase” of a shape-memory polymer, which could be simplified for the relaxation of cross linked shape-memory polymers to an SLS model. A slightly modified approach was introduced before by Tobushi et al. [26]. It should be noted that all these models were focused on the prediction of the changes of viscoelastic behaviour with temperature. In contrast, the target of our present work was the development of a simple kinetic approach for a prediction of the complete recovery behaviour including recovery times and recovery rates. Here we could demonstrate that a standard SLS model is suitable for description of the shape recovery behaviour of PEU obtained under stress-free conditions. A similar approach, where the recovery times of amorphous SMP were predicted on the basis of a Kelvin-Voigt element, was published recently by Bonner et al. [38].

The established model would provide a better understanding of the recovery kinetics of self sufficient actively moving PEU composite scaffolds. Moreover, it might form a knowledge-base for

development of other types of actively moving scaffolds in the future with an adjustable control on the recovery process to investigate the influence of stress/strain stimulation on the cell behaviour in short-time or long-term cell culture experiments.

Acknowledgements

This work was supported by Deutsche Forschungsgemeinschaft under grant No. SFB760, project B3.

Appendix. Supplementary data

A table with best fit parameter values for stress relaxation of PEU modeled with a Maxwell–Weichert model consisting out of three Maxwell units can be found in the online version of this article, at doi:10.1016/j.polymer.2010.10.051.

References

[1] Behl M, Lendlein A. Materials Today 2007;10(4):20–8.
[2] Behl M, Zotzmann J, Lendlein A. Advances in Polymer Science 2010;226:1–40.
[3] Mather PT, Luo XF, Rousseau IA. Annual Review of Materials Research 2009;39:445–71.
[4] Ratna D, Karger-Kocsis J. Journal of Materials Science 2008;43(1):254–69.
[5] Behl M, Lendlein A. Soft Matter 2007;3:58–67.
[6] Lendlein A, Kelch S. Materials Science Forum 2005;492-493:219–24.
[7] Behl M, Lendlein A. Journal of Materials Chemistry 2010;20(17):3335–45.
[8] Kolesov IS, Radusch H-J. Express Polymer Letters 2008;2(7):461–73.
[9] Xie T. Nature 2010;464(7286):267–70.
[10] Wagermaier W, Kratz K, Heuchel M, Lendlein A. Advances in Polymer Science 2010;226:97–145.
[11] Kelch S, Steuer S, Schmidt AM, Lendlein A. Biomacromolecules 2007;8(3):1018–27.
[12] Kim BK, Lee SY, Xu M. Polymer 1996;37(26):5781–93.
[13] Kolesov IS, Kratz K, Lendlein A, Radusch H-J. Polymer 2009;50(23):5490–8.
[14] Lin JR, Chen LW. Journal of Applied Polymer Science 1998;69(8):1575–86.
[15] Behl M, Ridder U, Feng Y, Kelch S, Lendlein A. Soft Matter 2009;5(3):676–84.
[16] Wang LS, Chen HC, Xiong ZC, Pang XB, Xiong CD. Materials Letters 2010;64(3):284–6.
[17] Zhang H, Wang H, Zhong W, Du Q. Polymer 2009;50(6):1596–601.
[18] Atli B, Gandhi F, Karst G. Proceedings of SPIE-The International Society for Optical Engineering 2007;6524(Electroactive Polymer Actuators and Devices (EAPAD) 2007), pp. 65241S/65241–65241S/65210.
[19] Cui J, Kratz K, Lendlein A. Smart Materials & Structures 2010;19:065019.
[20] Cui J, Kratz K, Heuchel M, Hiebl B, Lendlein A. Polymers for Advanced Technologies; 2010. doi:10.1002/pat.1733 [published online on 15.07.2010].
[21] Khonakdar HA, Jafari SH, Rasouli S, Morshedian J, Abedini H. Macromolecular Theory and Simulations 2007;16(1):43–52.
[22] Miaudet P, Derre A, Maugey M, Zakri C, Piccione PM, Inoubli R, Poulin P. Science 2007;318(5854):1294–6.
[23] Choi NY, Lendlein A. Soft Matter 2007;3(7):901–9.
[24] Diani J, Liu YP, Gall K. Polymer Engineering and Science 2006;46(4):486–92.
[25] Liu YP, Gall K, Dunn ML, Greenberg AR, Diani J. International Journal of Plasticity 2006;22(2):279–313.
[26] Tobushi H, Hashimoto T, Hayashi S, Yamada E. Journal of Intelligent Material Systems and Structures 1997;8(8):711–8.
[27] Barot G, Rao IJ. Zeitschrift Fur Angewandte Mathematik Und Physik 2006;57(4):652–81.
[28] Barot G, Rao IJ, Rajagopal KR. International Journal of Engineering Science 2008;46(4):325–51.
[29] Rao IJ. Proceedings of SPE-ANTEC; 2002 p.1936–1940.
[30] Sun L, Huang WM. Soft Matter 2010;6(18):4403–6.
[31] Kommareddy KP, Lange C, Rumpler M, Dunlop JWC, Manjubala I, Cui J, et al. Biointerphases 2010;5(2):45–52.
[32] Cui J, Kratz K, Lendlein A. Material Research Society Symposium Proceedings 2009;1190:93. doi:10.1557/PROC-1190-NN1503-1522.
[33] Mohr R, Kratz K, Weigel T, Lucka-Gabor M, Moneke M, Lendlein A. Proceedings of the National Academy of Sciences of the United States of America 2006;103(10):3540–5.
[34] Reddy S, Arzt E, del Campo A. Advanced Materials 2007;19(22):3833–7.
[35] Schmidt C, Neuking K, Eggeler G. Advanced Engineering Materials 2008;10(10):922–7.
[36] Ward IM, Sweeney J. An introduction to the mechanical properties of solid polymers. 2nd ed. Chichester: Wiley; 2004.
[37] Aklonis JJ, MacKnight WJ, Shen W. Introduction to polymer viscoelasticity. New York: Wiley & Sons; 1972.
[38] Bonner M, Montes de Oca H, Brown M, Ward IM. Polymer 2010;51(6):1432–6.
[39] Wineman AS, Rajagopal KR. Mechanical response of polymers. Cambridge: Cambridge University Press; 2000.